

# A novel pantothenate kinase gene (*PANK2*) is defective in Hallervorden-Spatz syndrome

Bing Zhou<sup>1</sup>, Shawn K. Westaway<sup>2</sup>, Barbara Levinson<sup>1</sup>, Monique A. Johnson<sup>2</sup>, Jane Gitschier<sup>1</sup> & Susan J. Hayflick<sup>2</sup>

Published online: 23 July 2001, DOI: 10.1038/ng572

Hallervorden-Spatz syndrome (HSS) is an autosomal recessive neurodegenerative disorder associated with iron accumulation in the brain. Clinical features include extrapyramidal dysfunction, onset in childhood, and a relentlessly progressive course<sup>1</sup>. Histologic study reveals iron deposits in the basal ganglia<sup>2</sup>. In this respect, HSS may serve as a model for complex neurodegenerative diseases, such as Parkinson disease<sup>3</sup>, Alzheimer disease<sup>4</sup>, Huntington disease<sup>5</sup> and human immunodeficiency virus (HIV) encephalopathy<sup>6</sup>, in which pathologic accumulation of iron in the brain is also observed. Thus, understanding the biochemical defect in HSS may provide key insights into the regulation of iron metabolism and its perturbation in this and other neurodegenerative diseases. Here we show that HSS is caused by a defect in a novel pantothenate kinase gene and propose a mechanism for oxidative stress in the pathophysiology of the disease.

HSS is a clinically heterogeneous group of disorders that includes classical disease with onset in the first two decades, dystonia, high globus pallidus iron with a characteristic radiographic appearance<sup>7</sup> and often either pigmentary retinopathy or optic atrophy. Atypical HSS is diagnosed in individuals who may not fit the diagnostic criteria for HSS<sup>1,2</sup> yet have radiographic or pathologic evidence of increased basal ganglia iron.

Using linkage analysis of an extended Amish pedigree, HS1, we previously defined an interval on chromosome 20p13 that contains the HSS gene<sup>8</sup>. We narrowed the HSS gene critical region by genotyping polymorphic microsatellite markers in families with classical HSS (Fig. 1). There was no evidence for a shared haplotype on disease chromosomes, which precluded our ability to refine the region further by linkage disequilibrium. The 1.4-Mb narrowed interval includes at least 21 known or predicted genes, most of which are expressed in brain (based on EST data). After analysis of 15 of these candidate genes, we observed a 7-bp deletion in the coding sequence in the

index family in a gene (here named *PANK2*) with homology to murine pantothenate kinase 1 (ref. 9). Sequencing of coding regions in other individuals with classical HSS confirms that HSS is due to mutations in *PANK2*. We found missense mutations resulting in nonconservative amino acid changes or null mutations in 32 of 38 individuals with classical HSS (Table 1 and Fig. 2b). Mutations on both alleles could be accounted for in 22 of these people.

We then examined DNA from people with atypical HSS and found *PANK2* mutations, all missense, in this group as well (Table 2). These individuals have later onset, and their diverse phenotypes include early-onset Parkinson disease, severe intermittent dystonia, stuttering with palilalia or facial tics with repetitive hair caressing; all have evidence of increased basal ganglia iron. In addition, we tested one consanguineous family (HS4) with pigmentary retinopathy and late-onset dystonia but without radiographic evidence of brain iron accumulation even into their thirties<sup>10</sup> and found a homozygous missense mutation. In the group studied, most mutations are unique, with the notable exception of a common Gly411→Arg (G411R) mutation, present in both classical and atypical individuals and not observed in 200 control chromosomes. The remaining reported mutations are unlikely to be polymorphisms because we did not see them in 150 ESTs associated with *PANK2* or in sequence from people already found to have two deleterious mutations.

Interestingly, atypical subjects HS61, HS62 and HS79 are compound heterozygotes for mutations for which classical subjects

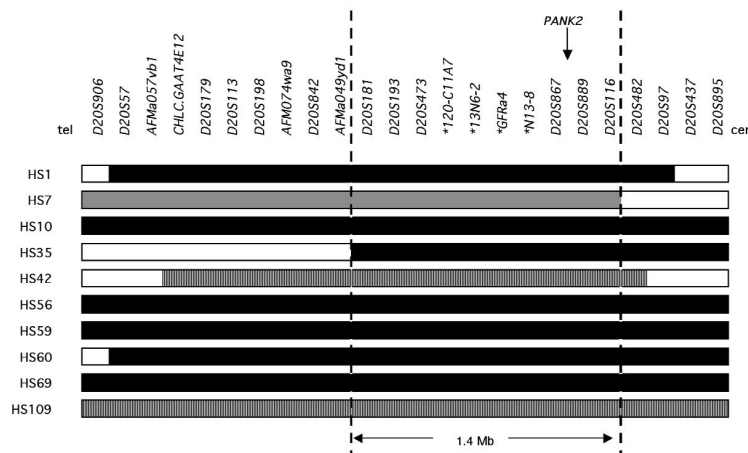


**Fig. 1** Localization of the HSS gene region. Markers used for genotyping are aligned from telomere to centromere; spacing is not to scale. Markers developed by the authors are indicated by \*. Data from families with classical HSS are summarized as follows: black rectangles indicate regions where markers are homozygous in families with known consanguinity, hatched rectangles indicate regions of homozygosity in families with no known consanguinity, and gray rectangles indicate regions included by recombination in nonconsanguineous families. Clear rectangles indicate excluded markers. The original candidate region defined by HS1 of ~3.3 Mb (ref. 8) was reduced by a recombination in family HS7 and a region of homozygosity in family HS35.

<sup>1</sup>Howard Hughes Medical Institute and Departments of Medicine and Pediatrics, University of California, Parnassus & Third Avenues, U-426, San Francisco, California 94143, USA. <sup>2</sup>Departments of Molecular and Medical Genetics, Pediatrics and Neurology, 3181 SW Sam Jackson Park Road, Oregon Health and Science University, Portland, Oregon 97201, USA. Correspondence should be addressed to S.J.H. (e-mail: hayflick@ohsu.edu).



## letter

Table 1 • *PANK2* mutations in classical HSS

Subject	Exon	Mutation	Result
HS1 <sup>a</sup>	2	627–633del <sup>b</sup>	frameshift
HS2	6	1261G→A	G411R
HS8	1C	270C→G	Y80X
	2	490C→T	R154W
HS10 <sup>a</sup>	1C	269insA <sup>b</sup>	Y80X
HS11	2	556C→T	R176C
	6	1261G→A	G411R
HS12	2	490C→T	R154W
	4	1112G→A	S361N
HS13	4	938T→C	L303P
HS23	6	1261G→A <sup>b</sup>	G411R
HS26	6	1261G→A	G411R
HS27	6	1283C→T <sup>b</sup>	T418M
HS35 <sup>a</sup>	3	876–877del <sup>b</sup>	frameshift
HS42 <sup>a</sup>	6	1261G→A <sup>b</sup>	G411R
HS56 <sup>a</sup>	6	1261G→A <sup>b</sup>	G411R
HS59 <sup>a</sup>	1C	245insA <sup>b</sup>	frameshift
HS60 <sup>a</sup>	2	680C→T <sup>b</sup>	T217I
HS63	2	544C→G	L172V
	6	1261G→A	G411R
HS66	3	824–852del	frameshift
HS67	5	1190T→C	I387T
HS69 <sup>a</sup>	6	IVS5-3C→G <sup>b</sup>	aberrant splicing exon 6
HS75	3	785–788del	frameshift
HS82 <sup>a</sup>	1C	148C→T <sup>b</sup>	Q40X
HS85	2	556C→T	R176C
HS101	6	1261G→A	G411R
HS109 <sup>a</sup>	6	1283C→T <sup>b</sup>	T418M
HS112	4	1051C→T	R341X
	6	1261G→A	G411R
HS115 <sup>a</sup>	2	636T→A <sup>b</sup>	C202X
HS118	6	1261G→A	G411R
HS124 <sup>a</sup>	5	1199A→T <sup>b</sup>	N390I
HS128 <sup>a</sup>	2	556C→T <sup>b</sup>	R176C
HS129 <sup>a</sup>	5	1201–1204dup <sup>b</sup>	frameshift
HS131	3	730A→T	K234X
HS133 <sup>a</sup>	4	1112G→A <sup>b</sup>	S361N

Survey of a large number of ESTs in the public database revealed none with the sequence changes described here. Numbers correspond to Fig. 2. X indicates stop. <sup>a</sup>Parents are known to be consanguineous or there is probable identity by descent based on haplotypes. <sup>b</sup>Mutation is homozygous. Individuals who are unlikely to be identical by descent and who appear to be homozygous for one mutation by sequence analysis may be hemizygous because of a deletion in one allele.

HS23, HS27, HS42, HS56 and HS109 are homozygous. This finding suggests interallelic complementation<sup>11</sup> and possible multimerization of *PANK2*. Although we do not know whether *PANK2* dimerizes, *Escherichia coli* pantothenate kinase has been shown to form a homodimer<sup>12</sup>.

Detailed sequence analysis reveals that *PANK2* is a member of a family of eukaryotic genes consisting of a group of six exons that encode homologous core proteins, preceded by a series of alternative initiating exons, some of which encode unique amino-terminal peptides. For example, by 5' RACE and EST analysis, we found evidence for at least five initiating exons for *PANK2*, but only one of these, exon 1C, has an open reading frame with potential initiation codons that splices in-frame to exon 2 (Fig. 2a). Moreover, we have identified three nonsense mutations within exon 1C in people with classical HSS (but not in controls; Table 1). We find a similar sequence in mouse, with homology in the derived amino acid sequence extending to the leucine codon at nucleotide 31 but diverging 5' of it. There is precedence for use of a leucine initiating codon in humans, which is probably read by a methionine tRNA<sup>13</sup>. The leucine

Table 2 • *PANK2* mutations in atypical HSS

Subject	Exon	Mutation	Result
HS4 <sup>a</sup>	3	751T→C <sup>b</sup>	S240P
HS20	6	1261G→A	G411R
HS38	2	400A→G	T124A
HS40	2	532C→T	R168C
	6	1261G→A	G411R
HS61	6	1261G→A	G411R
	6	1283C→T	T418M
HS62	6	1261G→A	G411R
	6	1283C→T	T418M
HS65	6	1261G→A	G411R
HS79	6	1261G→A	G411R
	6	1283C→T	T418M
HS113	3	764A→G	N245S
HS114	2	356G→T	G109V
	3	911A→T	N294I
HS134	2	400A→G	T124A
	6	1261G→A	G411R

Survey of a large number of ESTs in the public database revealed none with the sequence changes described here. Numbers correspond to Fig. 2. <sup>a</sup>Parents are known to be consanguineous or there is probable identity by descent based on haplotypes. <sup>b</sup>Mutation is homozygous.

codon is flanked by a reasonable initiation consensus sequence<sup>14</sup>. We also note the presence of a stem-loop structure (Fig. 2a) 14 nucleotides downstream from this leucine, the location of which has been shown to enhance translation initiation at nonconserved AUG or non-AUG initiation codons<sup>15</sup>. It is intriguing that the mouse stem-loop sequence is nearly identical, with only three nucleotide changes, two in the postulated loop of the stem-loop and one that changes a GC to a GU base pair, which implies structural conservation. Because of this strong conservation, we propose that the CUG may serve as an alternative initiation codon for translation in addition to one of the methionine codons downstream. We also note a 22-bp palindrome at the junction of spliced exons 1C and 2. This sequence may form a hairpin structure and thus explain why most *PANK2* ESTs terminate just 3' of the palindrome. We speculate that this sequence might serve a regulatory function. We note two polymorphisms in exon 1C: one at nucleotide 32 (T/A) that results in Leu/Gln, respectively, and the other at nucleotide 77 (G/C), resulting in Gly/Ala, respectively. Examination of public ESTs and our own sequencing efforts substantiate these polymorphisms.

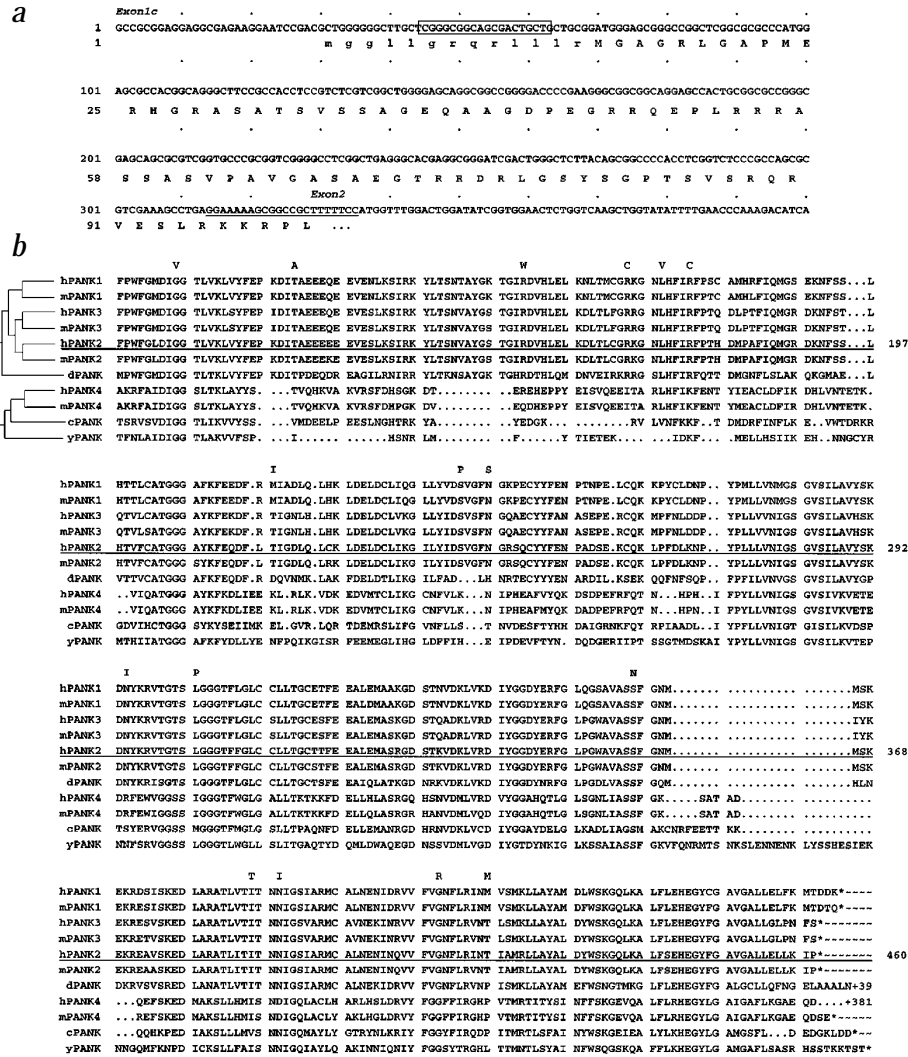
Alignment of the predicted core proteins (Fig. 2b) illustrates the relationship between the *PANK* sequences. Specifically, human *PANK1*, *PANK2* and *PANK3*, located on chromosomes 10q23, 20p13 and 5q35, respectively, are strikingly similar to their murine orthologs, with amino acid identity varying at most by only a few percent between orthologs and by approximately 20% among paralogs. We found a fourth mammalian pair of orthologs, with *PANK4* located on human chromosome 1p36, to be more similar to *Saccharomyces cerevisiae* and *Caenorhabditis elegans* sequences than to its mammalian homologs. Interestingly, the pantothenate kinase gene in *Drosophila* is quite similar to *PANK2*, a finding that is notable because the *Drosophila* pantothenate kinase hypomorphic mutant *fumble* shows neurologic incoordination, with impaired ability to climb, fly and mate<sup>16</sup> (K. Afshar, pers. comm.).

Differences in expression pattern among the *PANK* genes may explain why defects in *PANK2* lead to HSS. Although we find expression of *PANK1* in heart, liver and kidney, as described previously<sup>17</sup>, *PANK3* is expressed most abundantly in the liver (Fig. 3a). In contrast with these two genes, *PANK2* is expressed ubiquitously, including in retina and infant basal ganglia (data not shown).



**Fig. 2** Sequence of *PANK2* and comparison with other eukaryotic pantothenate kinase genes. **a**, *PANK2* cDNA sequence including exon 1C and the start of exon 2. The leucine codon CTG may serve as a codon for the initiating methionine, as described in the text. The 20-bp stem-loop structure downstream of this leucine is boxed. The 22-bp palindrome that spans exons 1C and 2 of the transcript is underlined. Nucleotides 32 and 77 are polymorphic (see text).

**b**, Alignment of the core amino acid sequences for pantothenate kinases from *Homo sapiens* (h), *Mus musculus* (m), *Drosophila melanogaster* (d), *C. elegans* (c) and *S. cerevisiae* (y). *PANK2* amino acid changes in HSS individuals are indicated above the sequence set. We obtained sequences by translating GenBank entries as follows: *hPANK1* was assembled from AL52532, AV718110, BG429406 and BF668178; *hPANK2* from AL353194, AL031670, BG397740 and AK021791; *hPANK3* from AK022961; *hPANK4* from AK001644; *mPANK1* from AF200357; *mPANK2* from AK016755; *mPANK3* assembled from ESTs BF140284 (corrected at two positions), BG083868 and BG070339; *mPANK4* assembled from ESTs BE554781, BG146074, AA671765 and BE982078; *dPANK* from AF221546; *cPANK* from AAB42246 (modified to include the final two exons); and *yPANK* from NP\_010820. We aligned the derived amino acid sequences with the Pileup algorithm from the Genetics Computer Group and plotted relatedness as indicated by the brackets. Amino acids of *hPANK2* are numbered consecutively from a to b and are underlined.



Expression of *PANK4* is most abundant in muscle, but it is expressed in all tissues. Quantity and cellular localization of each of these proteins may explain why *PANK2* mutations cause HSS.

Pantothenate kinase is an essential regulatory enzyme in coenzyme A (CoA) biosynthesis, catalyzing the cytosolic phosphorylation of pantothenate (vitamin B<sub>5</sub>), *N*-pantothenoyl-cysteine and pantotheine<sup>18</sup>. CoA is the major acyl carrier, playing a central role in intermediary and fatty acid metabolism. In both yeast and fly, each with only one pantothenate kinase gene, the null mutant is inviable<sup>16,19</sup>. Pantothenate kinase enzymatic activity has been found in the two eukaryotic proteins from this family studied to date<sup>9,20</sup>. Here we provide evidence for pantothenate kinase activity in *PANK2* by showing that the human gene *PANK2* can rescue the temperature-sensitive *E. coli* pantothenate kinase mutant<sup>21</sup> (Fig. 3b).

HSS is the first inborn error of pantothenate metabolism. We envision that the defects in HSS could result from product deficit and a secondary excess of metabolites downstream of the block. *PANK2* mutations are predicted to result in CoA depletion and defective membrane biosynthesis in those tissues in which this is the major pantothenate kinase or in those tissues with the greatest CoA demand. Rod photoreceptors continually generate membranous discs; hence, the retinopathy frequently observed in classical HSS may be secondary to this deficit. It may be possible

to therapeutically deliver phosphopantothenate or an alternative intermediary compound to cells in the affected tissues in order to bypass the enzymatic defect and drive CoA synthesis.

We also propose a mechanism of secondary metabolite accumulation as the cause of high iron concentration in the basal ganglia, the cardinal feature of this disorder. In normal brain, nonheme iron accumulates regionally and is highest in the medial globus pallidus and the substantia nigra pars reticulata<sup>22</sup>, the two regions most severely affected in HSS. Phosphopantothenate, the product of pantothenate kinase, normally condenses with cysteine in the next step in CoA synthesis. In HSS, phosphopantothenate is deficient, leading to cysteine accumulation, and *N*-pantothenoyl-cysteine and pantotheine will accumulate. High cysteine concentration has been found in the globus pallidus in HSS<sup>23</sup>. Cysteine undergoes rapid autooxidation in the presence of iron, which results in free radical production, and the cytotoxicity of cysteine is well-documented<sup>24</sup>. In turn, iron-induced lipid peroxidation, a likely mechanism of secondary pathogenesis in HSS<sup>23,25,26</sup>, is enhanced by free cysteine<sup>27,28</sup>, further stressing a cell with impaired membrane biosynthesis. Perturbed cysteine metabolism has been implicated in Parkinson and Alzheimer disease<sup>29</sup>. Thus, we propose that pantothenate metabolism may represent a common pathway implicated in neurodegeneration.

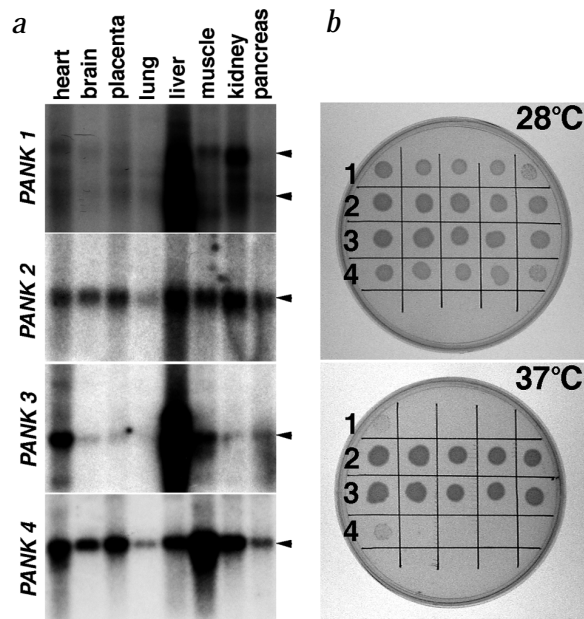


**Fig. 3** Expression and function of *PANK2*. **a**, Human tissue expression pattern of *PANK1*, *PANK2*, *PANK3* and *PANK4*. Arrows indicate the primary transcripts: *PANK1*, 1.8 kb, 3.0 kb; *PANK2*, 1.85 kb; *PANK3*, 1.65 kb; *PANK4*, 2.6 kb. **b**, *PANK2* rescue of an *E. coli* temperature-sensitive *coaA* mutant<sup>21</sup>. Strain ts9 grows poorly at 37°C, and at 28°C growth is only slightly affected. Rows 1 and 4 are independent clones, transfected with vector only; rows 2 and 3 are independent clones, transfected with plasmid containing human *PANK2*. Columns represent serial 1:10 dilutions from left to right.

Finally, in response to the unethical activities of Julius Hallervorden and Hugo Spatz during World War II (ref. 30), we propose a new name for HSS based on knowledge of the underlying biochemistry. We suggest that the group of disorders be known as pantothenate kinase associated neurodegeneration (PKAN).

## Methods

**Genotyping.** DNA was isolated from whole blood using standard procedures. Lymphoblast cell lines were established for some patients by EBV transformation. DNA was isolated from lymphoblast cell lines or from buccal brushings using the PUREGENE DNA Isolation Kit according to the manufacturer's instructions (Gentra Systems, Minneapolis, MN). Genomic DNA was amplified by the PCR using forward and reverse primers specific for each microsatellite repeat. PCRs (10–50 µl) contained 1×Taq Polymerase Buffer, 0.05 Units Taq Polymerase (Roche Biochemicals), 0.2 mM each dNTP, 0.5 mM spermidine or 5% DMSO, 0.5 µM forward and reverse primers, and 2 ng/µl genomic DNA template. PCRs were carried out using standard touchdown methods. PCR products were separated on 8% acrylamide (19:1 bisacrylamide:acrylamide), 5.6 M urea, 32% formamide, 1×TBE gels and blotted to Hybond™-N+ positively charged membranes (Amersham) according to methods published previously<sup>8</sup>, with the following exceptions: Blots were probed with digoxigenin-labeled repeat oligonucleotides, detected and developed using an Anti-Digoxigenin-Alkaline Phosphatase Antibody protocol (Roche).

**RACE.** To obtain full-length cDNA clones, we performed 5′- and 3′-RACE PCR with library AP1 or AP2 primers in conjunction with gene-specific primers (sequences available on request) from human testis and/or fetal brain Marathon-Ready cDNA libraries and the Marathon RACE kit according to the manufacturer's specifications (Clontech Laboratories, Inc.). Products were cloned into pT-Adv (Clontech) and plasmids were prepared (Qiagen). DNA sequencing was performed by the OHSU-MMI Research Core Facility (<http://www.ohsu.edu/core>), and sequence determination was performed on a model 377 Applied Biosystems Inc. automated fluorescence sequencer.

**Mutation detection.** Primers for sequence analysis of *PANC2* were chosen to amplify exons and their respective intron/exon boundaries after mapping cDNA sequence to genomic sequence. For mutation detection, PCR products were purified by NucleoSpin® Nucleic Acid Purification Kits (Clontech Laboratories, Inc.), quantitated, and sequenced using the same primers as for PCR amplification. Mutation screening of random populations was performed by PCR amplification of CEPH or locally obtained random DNA samples, followed by restriction digestion and resolution on polyacrylamide or agarose gels.

**Northern blotting.** A nylon membrane containing the RNA of several human tissues (Clontech) was incubated with <sup>32</sup>P-labeled probes derived from the highly divergent 3′-UTR sequences of the four human pantothenate kinase cDNAs. Hybridization was allowed to occur in PerfectHyb Plus (Sigma); hybridization and washing conditions were according to manufacturer's specifications.

**Complementation between *E. coli*.** *E. coli* strain ts9 (*leuB6 fluA2 lacY1 tsx-1 glnV44(AS) gal-6 LAM- hisG1(Fs) argG6 rpsL9 malT1 (LamR) xylA7 mtIA2 metB1 coaA1 ilu-1*) was obtained from the *E. coli* Genetic Stock Center, Yale University. Human *PANK2* core cDNA was PCR amplified and cloned into BamHI/SalI of pQE-80L (Qiagen). The resulting construct was introduced into ts9 *E. coli* by standard CaCl<sub>2</sub> transformation, selected with ampicillin, serially diluted and incubated at the appropriate temperature.

## Acknowledgments

We are grateful to the many individuals, families and clinicians (J.P. Harpey, M. Shevell, M. Piñeda, G. Kurlmann, J. Coppeto, J. Jankovic, S. Davis, H. Hattori, K. Sethi, M. Pandolfo, L. Angelini, N. Nardocci, A. Malandrini, J. Penzien, G. Mortier, M. Hoeltzenbein, J.A. Urtizberea, M.A.M. Salih, D. Buckley, C. Haeggeli, A. Bottani, B. Beinlich, J. Østergaard, S. Bunday, F. Stogbauer, K. Nørgaard Hansen, J. Guimarães, C. Yalcinkaya, A. Feigenbaum, Z. Liptai, J. Carlo, P. Blasco, A. Zimmerman, R. Cilio, E. Bertini, G. Worley, U. Thyen, J. Molineuvo, M. Melis, G. Cossu, J. Menkes, K. Hollódy, A. Barrett, S. Simpson, C. Schrander-Stumpel, H. Chaabouni, R. Gatti, H. Topaloglu, M. Nigro, F. Hisama, N.R.M. Buist, B. Ben-Ze'ev, A. Macaya, B. Korf, P. Heydemann, S. Abbs, R. Robinson, L. Shinobu, E. Dooling, P. Wheeler, P. Rosman, W. Wasiewski, P. Castelnaud, P. Evrard, R. Haslam, M. Filocamo, M. Karwacki, T. Kmiec, S. Frucht, T. Konishi, M. Regina Reyes, M. Al-Mateen, K. Weidenheim, M. Delgado, S. Johnsen, S. Golembowski, W. Ondo, S. Bohlega, R. Bustamante, O. Fernandez, M. Wiznitzer, H. Morgan, I. Butler, T. Babb, D. Sanderson, M. Williams, C. Harding, R. Steiner, S. Toor, E. Thompson, J. MacKenzie, J. Clyman and D. Fornoff) who contributed to this study. We thank T. Taylor, H. Payami, M. Litt, A. Malone, S. Bae, M. Gunthorpe, H. Consenigo, E. Stewart, S. Packman, the Oregon Health and Science University MMI Sequencing Core, and the Hallervorden-Spatz Syndrome Association. This work was supported by a grant from the National Eye Institute and the Sandler Neurogenetics Center at the University of California, San Francisco. J.G. is an investigator with the Howard Hughes Medical Institute.

Received 14 May; accepted 27 June 2001.

- Dooling, E.C., Schoene, W.C. & Richardson, E.P. Jr. Hallervorden-Spatz syndrome. *Arch. Neurol.* **30**, 70–83 (1974).
- Swaiman, K.F. Hallervorden-Spatz syndrome and brain iron metabolism. *Arch. Neurol.* **48**, 1285–1293 (1991).
- Sofic, E. et al. Increased iron III and total iron content in postmortem substantia nigra in parkinsonian brain. *J. Neural Trans.* **74**, 199–205 (1988).
- Connor, J.R., Snyder, B.S., Beard, J.L., Fine, R.E. & Mufson, E.J. Regional distribution of iron and iron regulatory proteins in the brain in aging and Alzheimer's disease. *J. Neurosci. Res.* **31**, 327–335 (1992).
- Dexter, D.T. et al. Alterations in the levels of iron, ferritin and other trace metals in Parkinson's disease and other neurodegenerative diseases affecting basal ganglia. *Brain* **114**, 1953–1975 (1991).
- Miszkiel, K.A. et al. The measurement of R-2, R-2-\* and R-2' in HIV-infected patients using the prime sequence as a measure of brain iron deposition. *Magn. Reson. Imaging* **15**, 1113–1119 (1997).
- Angelini, L. et al. Hallervorden-Spatz disease: clinical and MRI study of 11 cases diagnosed in life. *J. Neurol.* **239**, 417–425 (1992).
- Taylor, T.D. et al. Homozygosity mapping of Hallervorden-Spatz syndrome to chromosome 20p12.3–p13. *Nature Genet.* **14**, 479–481 (1996).
- Rock, C.O., Calder, R.B., Karim, M.A. & Jackowski, S. Pantothenate kinase regulation of the intracellular concentration of coenzyme A. *J. Biol. Chem.* **275**, 1377–1383 (2000).
- Coppeto, J.R. & Lessell, S. A familial syndrome of dystonia, blepharospasm, and pigmentary retinopathy. *Neurology* **40**, 1359–1363 (1990).



11. Gravel, R.A. *et al.* Mutations participating in interallelic complementation in propionic acidemia. *Am. J. Hum. Genet.* **55**, 51–58 (1994).
12. Yun, M. *et al.* Structural basis for the feedback regulation of *Escherichia coli* pantothenate kinase by coenzyme A. *J. Biol. Chem.* **275**, 28093–28099 (2000).
13. Blackwood, E.M. *et al.* Functional analysis of the AUG- and CUG-initiated forms of the c-Myc protein. *Mol. Biol. Cell* **5**, 597–609 (1994).
14. Kozak, M. The scanning model for translation: an update. *J. Cell Biol.* **108**, 229–241 (1989).
15. Kozak, M. Downstream secondary structure facilitates recognition of initiator codons by eukaryotic ribosomes. *Proc. Natl. Acad. Sci. USA* **87**, 8301–8305 (1990).
16. Afshar, K., Gonczy, P., DiNardo, S. & Wasserman, S.A. fumble encodes a pantothenate kinase homolog required for proper mitosis and meiosis in *Drosophila melanogaster*. *Genetics* **157**, 1267–1276 (2001).
17. Karim, M.A., Valentine, V.A. & Jackowski, S. Human pantothenate kinase 1 (PANK1) gene: Characterization of the cDNAs, structural organization and mapping of the locus to chromosome 10q23.2-23.31. *Am. J. Hum. Genet.* **67**, A984 (2000).
18. Abiko, Y. Investigations on pantothenic acid and its related compounds. IX. Biochemical studies. 4. Separation and substrate specificity of pantothenate kinase and phosphopantothenoylcysteine synthetase. *J. Biochem. (Tokyo)* **61**, 290–299 (1967).
19. Winzeler, E.A. *et al.* Functional characterization of the *S. cerevisiae* genome by gene deletion and parallel analysis. *Science* **285**, 901–906 (1999).
20. Calder, R.B. *et al.* Cloning and characterization of a eukaryotic pantothenate kinase gene (panK) from *Aspergillus nidulans*. *J. Biol. Chem.* **274**, 2014–2020 (1999).
21. Vallari, D.S. & Rock, C.O. Isolation and characterization of temperature-sensitive pantothenate kinase (coaA) mutants of *Escherichia coli*. *J. Bacteriol.* **169**, 5795–5800 (1987).
22. Hill, J.M. & Switzer, R.C. III. The regional distribution and cellular localization of iron in the rat brain. *Neuroscience* **11**, 595–603 (1984).
23. Perry, T.L. *et al.* Hallervorden-Spatz disease: cysteine accumulation and cysteine dioxygenase deficiency in the globus pallidus. *Ann. Neurol.* **18**, 482–489 (1985).
24. Yoon, S.J., Koh, Y.H., Floyd, R.A. & Park, J.W. Copper, zinc superoxide dismutase enhances DNA damage and mutagenicity induced by cysteine/iron. *Mutat. Res.* **448**, 97–104 (2000).
25. Park, B.E., Netsky, M.G. & Betsill, W.L. Jr. Pathogenesis of pigment and spheroid formation in Hallervorden-Spatz syndrome and related disorders. *Neurology* **25**, 1172–1178 (1975).
26. Tripathi, R.C., Tripathi, B.J., Bauserman, S.C. & Park, J.K. Clinicopathologic correlation and pathogenesis of ocular and central nervous system manifestations in Hallervorden-Spatz syndrome. *Acta Neuropathol.* **83**, 113–119 (1992).
27. Searle, A.J. & Willson, R.L. Stimulation of microsomal lipid peroxidation by iron and cysteine. Characterization and the role of free radicals. *Biochem. J.* **212**, 549–554 (1983).
28. Yang, E.Y., Campbell, A. & Bondy, S.C. Configuration of thiols dictates their ability to promote iron-induced reactive oxygen species generation. *Redox. Rep.* **5**, 371–375 (2000).
29. Heafield, M.T. *et al.* Plasma cysteine and sulphate levels in patients with motor neurone, Parkinson's and Alzheimer's disease. *Neurosci. Lett.* **110**, 216–220 (1990).
30. Shevell, M. Racial hygiene, active euthanasia, and Julius Hallervorden [see comments]. *Neurology* **42**, 2214–2219 (1992).